Stability Analysis of a Plane, Rectangular, Boron–epoxy Laminated Plate Basing on Strength Properties Determined by Different Methods

Andrzej Mróz

Technical University of Lodz
Faculty of Mechanical Engineering
Technical University of Łódź,
Stefanowskiego 1/15, Łódź, Poland

This paper presents the examples of practical applications of composite materials in mechanical engineering and methods in determining of micromechanical properties of a laminate, corresponding to a plate, made of epoxy matrix strengthened with longitudinal boron fibres, including:

1. Strength of Materials equations

2. Halphin–Tsai equations

3. Theory of elasticity

Basing on determined micromechanical properties, numerical analysis of stability (of rectangular, composite plate, simply supported on all edges, axially compressed) using Finite Element Method (Ansys program) is carried through. First four buckling modes are presented and compared to the corresponding ones for isotropic model (steel).

Keywords: Boron–epoxy Composites, Strength of materials, Halphin–Tsai, Elasticity, Stability

1. Application of composite materials

Nowadays, in the times of rapid development in modern computer technologies and production optimization, it is desirable to use strength properties of available construction materials optimmally. The main reason for this operation, in the area of massive production systems is the maximization of the savings resulting from reduction of the material amount (mass reduction of the detail) in manufactured batch, assuring both safety and reliability level respectively. Remarkable domains, in which this phenomena is observed are the air and motor industries.

Figure 1 An aeroplane as an example of a composite structure [1]

The choice of the material used in the production depends on many factors. The most important of them are those defining the value and the type of the loading and working conditions. Today, the most popular construction materials are the cast iron, steel, aluminium and their alloys. The main advantages of using them are high mechanical properties, relatively low cost and general accessibility. In the drawbacks, high density[1] and low corrosion resistance should be mentioned.

Mass reduction of the element plays superior role in the design stage of the vehicles in different means of transport. For instance, it is difficult to imagine the airplane completely made of steel parts, which weight would not let even taking off. It is estimated, that reduction of mass of approximately 0,5 kg bears the fuel savings of 1400 litres per year [2].

For this reason, the engineers– designers are searching for new (ultralight) materials, possesing required strength properties. These materials are called the composites, and are commonly used in construction elements in the plane (Fig. 1), space vehicles, as parts in combustion engines (connecting rods, pistons, cylinder sleeves), in sport equipment (tennis rackets, golf clubs), in medicine (dentist implantation, vein stenters) and angling (fishing rods, boats).

Except for required mechanical properties, composites are corrosion resistant. For instance, in the fifties of XX–st century, in VFB Sachsenring Automobilwerke factory, an innovatory automobile vehicle model was designed and produced in the 40 years long period. Worth mentioning is the fact, that a new, polymer (made of hardening plastics) body was used in this model.

This solution was to increase both corrosion resistance and safety level (higher impact stength and non-flammable body) by simultaneous reduction of the total vehicle mass (only 19kW drive motors were used). Trabant (Fig. 2), popularly called as "Trabi" or "Trabbi" turned out to be a very reliable and cheap project. Finally, almost 3 million copies were manufactured and for this reason it is referred to be a "cult" project[2].

---

[1]steel type S235JRG2 according to DIN EN 1.0025 (7,86 g/cm^3)

[2]in 2009, after 10 years long stoppage in production, a new, electric driven Trabant NT model was presented Trabant nT

Figure 2 Trabant- an innovative composite body [3]

2.   Strength properties of boron fibres and epoxy matrix

Composite, as homogeneous structural material is composed of at least two components, closely connected with each other on the macroscope level and are not insoluble in each other[3].

Composite materials occur in natural environment. The wooden trunk structure is the most remarkable composite example (it is composed of particular structures: bark, cambium, alburnum, duramen, pith). Generally, the composites can be classified in three cathegories:

1. composite strenghtened with heterogeneous particles, e.g. concrete (cement + sand)

2. flake composite, e.g. wooden plywood

3. composite strengtened with the fibres, e.g. glass-epoxy laminate

A singular lamina of considered composite is composed of longitudinally packed boron fibres (with tungsten core) in the matrix made of epoxy. The strength properties for epoxy (isotropic material) is presented in Tab. 1 and boron fibres in Tab. 2.

Table 1 Strength properties of boron fibres [5]

| Young's modulus	3.4 GPa
Poisson's ratio	0.3
shear modulus	1.3 GPa
tensile strength	72 MPa
compressive strength	102 MPa
shear strength	34 MPa
specific density	1200 kg/m^3

---

[3]it is equivalent to assumption, that strenghtening phases (fibres) and bonding phases (matrix) can be specified

Table 2 Strength properties of epoxy matrix [4]

axial modulus	380 GPa
axial Poisson's ratio	0.13
specific density	2600 kg/m^3

According to characteristic strength properties and structure, boron fibres have been studied in detailed tests and model analysis by NASA and Boeing Corporation [6], [7]. The access to literature is limited (due to encryption of reports) and mainly comes from the seventies of the previous century.

A single boron fibre is composed of the 10μm wide tungsten core and boron coating, which is applied by the diffusion method[4]. The total diameter of the fiber is about 140μm. The boron–fibre's cross–section and external surface are presented in Fig. 3 and Fig. 4.
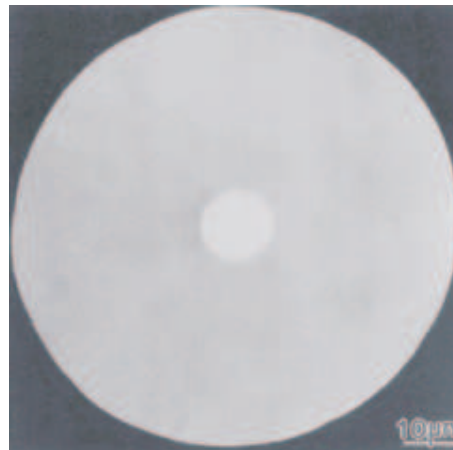
Figure 3 Boron fibre cross–section [5]

Figure 4 The external surface of the fiber [5]

---

[4]this means, that the structure of the fiber is not homogeneous (but composite)

Boron–epoxy composites have been widely used in the air industry (as the plated elements in the airplane F–111, which is presented in Fig. 5) and space vehicles. In [6] an analysis of the boron–epoxy composites used as a repair kit for damaged parts of construction was carried through.

Figure 5 RAAF F111 [8]

The production process of the composites is very costful, and for this reason this material is not so popular as glass–epoxy laminates. The technological develepoment, which leads to the discovery of superstrong materials, again has directed the scientists' interest to boron fibres in aluminium matrix. In this way a new composite has been explored in detail (the tensile strength 2000MPa [8]).

The content analysis of the tested boron–epoxy composite is detailed in Tab. 3.

Table 3 The content analysis in the boron-epoxy composite [4], [5]

The fibrous volume fraction factor:	80
Fiber's diameter d:	0,142 mm
Distance between the fibers:	0,151 mm
Density of the fibers:	2600 kg/m^3
Density of the matrix:	1200 kg/m^3
Density of the composite:	2320 kg/m^3
Volume of 1kg composite:	4,31x10-4 m^3
Fibrous volume in 1 kg of the composite:	3,45x10-4 m^3
Matrice's volume in 1 kg of the composite:	0,86x10-4 m^3
Mass of the fibers in 1 kg of the composite:	0,897 kg
Mass of the matrix in 1 kg of the composite:	0,103 kg

3.   Determination of the strength properties

3.1.   *Strength of materials equations*

The following equations in this section refer to [10].

- **Volume fractions**

  $V_1 = 0.8$ - fibrous volume fraction

  $V_2 = 0.2$ - matrix volume fraction

- **Longitudinal Young's Modulus** E_{11} Regarding the values from Tab. 1 and Tab. 2: $E_1 = 380$ [GPa] – Axial modulus of the fibers

  $E_2 = 3.4$ [GPa] – Axial modulus of the matrix

  Using the rule of mixture:

  $$E_{11} = V_1 E_1 + V_2 E_2 \tag{1}$$

  we get longitudinal (axial) Young's modulus of the composite:
  $E_{11} = 304.7$ [GPa]

- **Transverse Young's Modulus** E_{22}

  $$\frac{1}{E_{22}} = \frac{V_1}{E_1} + \frac{V_2}{E_2} \tag{2}$$

  $E_{22} = 16.1$ [GPa]

- **Major Poisson's ratio** ν_{12}

  $\nu_1 = 0.13$ - axial Poisson's ratio of the fibers

  $\nu_2 = 0.3$ - axial Poisson's ratio of the matrix

  Including equation from [4]:

  $$\nu_{12} = V_1 \nu_1 + V_2 \nu_2 \tag{3}$$

  $\nu_{12} = 0.164$

- **Minor Poisson's ratio** ν_{21}

  $$\nu_{21} E_{11} = \nu_{12} E_{22}, \qquad \nu_{21} = 8.8310^{-4} \tag{4}$$

- **In–plane Shear Modulus** G_{12}

  G_1 - shear modulus of the fibers

  $$G_1 = \frac{E_1}{2(1 + \nu_1)}, \qquad G_1 = 168.1[GPa] \tag{5}$$

  G_2 - shear modulus of the matrix

$$G_2 = \frac{E_2}{2(1 + \nu_2)}, \qquad G_2 = 1.3[\text{GPa}] \tag{6}$$

Using equations (5) and (6):

$$\frac{1}{G_{12}} = \frac{V_1}{G_1} + \frac{V_2}{G_2} \tag{7}$$

we finally get:

$G_{12} = 6.3$ [GPa]

3.2. *Halphin–Tsai equations*

For higher values ($> 70\%$ of fibrous volume fraction factor), the properties determined in Strength of Materials equations differ much from the experimental data. In order to describe them more precisely, Halphin–Tsai criterion should be used. More detailed description can be found in [11].

- **Longitudinal Young's Modulus** E_{11}

  Referring to (1) we get:

  $E_{11} = 304.7[GPa]$

- **Transverse Young's Modulus** E_{22} [4]

  $\xi = 2$ – increment factor [4] (for hexagonal layout and circular fibrous cross–section presented in Fig. 6 and Fig. 7)
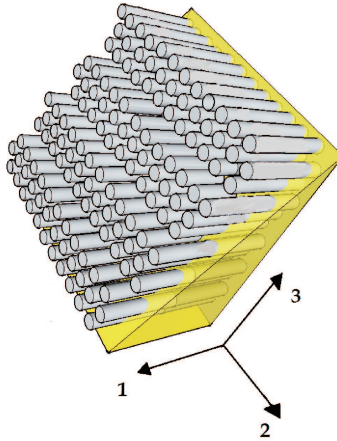

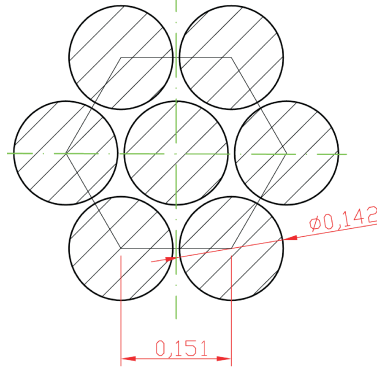**Figure 6** Layout–diagram of the fibers in the composite

Figure 7 Hexagonal layout in the composite

$$\eta = \frac{\frac{E_1}{E_2} - 1}{\xi + \frac{E_1}{E_2}} \tag{8}$$

hence $\eta = 0.974$

$$E_{22} = E_2 \frac{1 + (\xi \eta V_1)}{1 - \eta V_1} \tag{9}$$

finally we get: $E_{22} = 39.3$ [GPa]

- **Major Poisson's ratio ν_{12}**
  Referring to (3) we get:

  $\nu_{12} = 0.164$

- **Minor Poisson's ratio ν_{21}**
  Using (4) we get:

  $\nu_{21} = 0.021$

- **In–plane Shear Modulus G_{12}[11]**
  $\lambda = 1$ – increment factor (for hexagonal layout and circular fibrous cross–section) Using the relations (5) and (6):

$$\zeta = \frac{G_1/G_2 + 1}{G_1/G_2 - \lambda} \tag{10}$$
$$\zeta = 0.985$$
$$G_{12} = G_2 \frac{1 + (\zeta \lambda V_1)}{1 - \zeta V_1} \tag{11}$$
$$G_{12} = 11.0 \text{[GPa]}$$

For higher values of fibrous volume fraction factors ($> 50\%$), it is strongly recommended to use Hewitt's and Mahelbre's equations in order to determine the increment factor [4]:

$$\lambda = 1 + 40V_f^{10} \tag{12}$$

Using the equations (10) and (11) we finally get:

$G_{12} = 27.7$ [GPa]

3.3. *Theory of Elasticity Equations*

The following equations in this subsection are described in [4].

- **Longitudinal Young's Modulus E_{11}**

$$E_{11} = \kappa_1 - \frac{\kappa_2}{\kappa_3 + \kappa_4} \tag{13}$$

$$\kappa_1 = E_1 V_1 + E_2 V_2 \tag{14}$$

$$\kappa_2 = 2E_1 E_2 V_1 V_2 (\nu_1 - \nu_2)^2 \tag{15}$$

$$\kappa_3 = E_1 (2V_1 \nu_2^2 - \nu_2 + V_1 \nu_2 - V_1 - 1) \tag{16}$$

$$\kappa_4 = E_2 (-1 - 2V_1 \nu_1^2 + \nu_1 - V_1 \nu_1 + 2\nu_1^2 + V_1) \tag{17}$$

finally:$E_{11} = 304.7$ [GPa]

- **Major Poisson's ratio ν_{12}**

The value of the Major Poisson's ratio ν_{12}

$$\nu_{12} = \nu_1 V_1 + \nu_2 V_2 + \frac{\eta_1}{\eta_2 + \eta_3} \tag{18}$$

$$\eta_1 = V_1 V_2 (\nu_1 - \nu_2)[2E_1(\nu_2)^2 + \nu_2 E_1 - E_1 \tag{19}$$

$$+ E_2 - E_2 \nu_1 - 2E_2(\nu_1)^2]$$

$$\eta_2 = E_1[2V_1(\nu_2)^2 - \nu_2 + \nu_2 V_1 - 1 - V_1] \tag{20}$$

$$\eta_3 = E_2[2(\nu_1)^2 - \nu_1 V_1 - 2(\nu_1)^2 V_1 + V_1 - 1 + \nu_1] \tag{21}$$

$$\nu_{12} = 0.156$$

- **Transverse Young's Modulus E_{22}**

In order to determine E_{22}, the values of G_{23} and ν_{23} must be evaluated first.

$$E_{22} = 2(1 + \nu_{23})G_{23} \tag{22}$$

$$K_1 = \frac{E_1}{2(1 + \nu_1)(1 - 2\nu_1)} \tag{23}$$

$$K_2 = \frac{E_2}{2(1 + \nu_2)(1 - 2\nu_2)} \tag{24}$$

$$K = \frac{K_2(K_1 + G_2)V_2 + K_1(K_2 + G_2)V_1}{(K_1 + G_2)V_2 + (K_2 + G_2)V_1} \tag{25}$$

$$K = 5.368 \text{ [GPa]}$$

Introducing parameters as below:

$$A = A_1 + A_2 A_3 \tag{26}$$

$$A_1 = 3V_1(1 - V_1)^2 \left(\frac{G_1}{G_2} - 1\right)\left(\frac{G_1}{G_2} + \mu_1\right) \tag{27}$$

$$A_2 = \frac{G_1}{G_2}\mu_2 + \mu_1\mu_2 - (\frac{\mu_2 G_1}{G_2} - \mu_1)V_1^3 \tag{28}$$

$$A_3 = V_1\mu_2(\frac{G_1}{G_2} - 1) - \left(\frac{\mu_2 G_1}{G_2} + 1\right) \tag{29}$$

$$B = B_1 + B_2 B_3 + B_4 \tag{30}$$

$$B_1 = -3V_1(1 - V_1)^2 \left(\frac{G_1}{G_2} - 1\right)\left(\frac{G_1}{G_2} + \mu_1\right) \tag{31}$$

$$B_2 = 0.5\left[\mu_2\frac{G_1}{G_2} + \left(\frac{G_1}{G_2} - 1\right)V_1 + 1\right] \tag{32}$$

$$B_3 = (\mu_2 - 1)\left(\frac{G_1}{G_2} + \mu_1\right) - 2\left(\mu_2\frac{G_1}{G_2} - \mu_1\right)V_1^3 \tag{33}$$

$$B_4 = 0.5\left[V_1(\mu_2 + 1)\left(\frac{G_1}{G_2} - 1\right)\left(\frac{G_1}{G_2} + \mu_1 + \frac{\mu_2 G_1}{G_2} - \mu_1\right)V_1^3\right] \tag{34}$$

$$C = C_1 + C_2 + C_3 \tag{35}$$

$$C_1 = 3V_1(1 - V_1)^2 \left(\frac{G_1}{G_2} - 1\right)\left(\frac{G_1}{G_2} + \mu_1\right) \tag{36}$$

$$C_2 = \mu_2\frac{G_1}{G_2} + \left(\frac{G_1}{G_2} - 1\right)V_1 + 1 \tag{37}$$

$$C_3 = \frac{G_1}{G_2} + \mu_1 + \left(\frac{\mu_2 G_1}{G_2} - \mu_1\right)V_1^3 \tag{38}$$

and solving the equation(only the positive value is correct):

$$f(x) = Ax^2 + 2Bx + C = 0 \tag{39}$$

where:

$$x = \frac{G_{23}}{G_2} \tag{40}$$

we get: $G_{23} = 7.75$ [GPa]

$$m = 1 + 4K\frac{\nu_{12}^2}{E_{11}} \qquad m = 1.002 \tag{41}$$

$$\nu_{23} = \frac{K - mG_{23}}{K + mG_{23}} \qquad \nu_{23} = -0.182 \tag{42}$$

finally: $E_{22} = 12.7$ [GPa]

- **Minor Poisson's Ratio ν_{21}**

  Using the (4) we get:

  $\nu_{21} = 6.483 10^{-3}$

- **In–plane Shear Modulus G_{12}**

$$G_{12} = G_2\frac{G_1(1 + V_1) + G_2(1 - V_1)}{G_1(1 - V_1) + G_2(1 + V_1)} \tag{43}$$
$$G_{12} = 11.0 [\text{GPa}]$$

The determined strength parameters can be compared in the below table[5]:

Table 4 Summarizing statement of determined strength properties of considered material

		Strength of materials Equations	Halphin-Tsai Equations	Theory of Elasticity Equations
E_{11}:	GPa	304.7	304.7	304.7
E_{22}:	GPa	16.1	39.3	12.7
ν_{12}:	-	0.164	0.164	0.156
ν_{21}:	-	0.008	0.021	0.065
G_{12}:	GPa	6.3	27.7	11.0

4. Analytical determination of buckling load

4.1. *Isotropic Material*

The buckling force for isotropic plate (width $a = 500$ mm, length $b = 500$ mm, thickness $h = 5$ mm, number of halfwaves in the compression direction $m = 1$) is described in literature [12] as:

$$N_{cr} = \frac{\pi^2 D}{a}(m + \frac{1}{m}\frac{a^2}{b^2})^2 \tag{44}$$

$$D = \frac{Eh^3}{12(1 - \nu^2)} \tag{45}$$

and the buckling stress is equal to: $\sigma_{cr} = 75.9$ [MPa]

---

[5]Halphin–Tsai in–plane Shear Modulus according to Hewitt's and Mahelbre's Equations

4.2. *Orthotropic Material*

The buckling load for the compressed orthotropic plate is described by equation below [10]:

$$\sigma_{cr} = \frac{\pi^2 D_{red}}{b^2} \tag{46}$$

where:

$$D_w = \frac{G_{12}h^3}{12} \tag{47}$$

$$\tag{48}$$

$$D_1 = \frac{E_{11}h^3}{12(1 - \nu_{12}\nu_{21})} \tag{49}$$

$$D_2 = \frac{E_{22}h^3}{12(1 - \nu_{12}\nu_{21})} \tag{50}$$

$$D_{red} = D_1 + D_2 + D_1\nu_2 + D_2\nu_1 + 4D_w \tag{51}$$

Table 5 Summarizing statement of analytical buckling stress values

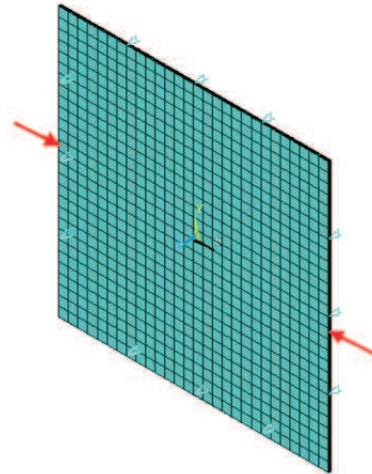|	unit	Strength of materials equations	Halphin-Tsai equations	Theory of Elasticity equations
σ_{cr}:	MPa	28.9	38.6	31.8

Figure 8 Loading and initial conditions

5.   Numerical analysis of tested composite plate

Knowing the strength parameters of boron–epoxy composite, numerical analysis of the buckling process was carried through. The program used to computer simulation was ANSYS (R) Release 11.0SP1.

The object of the numerical analysis is a rectangular, simply supported on all edges plate (width: 500 mm, length: 500 mm, thickness: 5 mm). The composite is made of 25 parallel to compression load, unidirectional layers (0.2 mm thick each of them).

The material of the plate was boron–epoxy laminate which is treated as an orthotropic material (the properties were determined in sec 3). Refering to Ansys documentation it is recommended to use shell type of the elements (it is possible to modify the ply angles). In this analysis SHELL 99 type of the element was used.

Refering to [13] SHELL99 may be used for layered applications of a structural shell model. The element has six degrees of freedom at each node: translations in the nodal x, y, and z directions and rotations about the nodal x, y, and z–axes. The element is defined by eight nodes, average or corner layer thicknesses, layer material direction angles, and orthotropic material properties.

After creating the geometry, the model was meshed using mapped method. The plate is simply supported on all edges and is axially compressed (along x–axis) with elementary pressure value (Fig. 8). The critical load is determined by eigen–value modal analysis.

5.1.   *Material properties*

The material properties used in numerical calculations are determined by:

1. Strength of Materials equations

2. Halphin–Tsai equations

3. Theory of elasticity

and are listed in Tab. 4. For isotropic material, the values of Young's modulus and Poisson's ratio correspond to steel and are equal to: $E = 210$ [GPa], $\nu = 0.3$.

5.2.   *First buckling mode*

The first buckling mode form of the composite plate (Fig. 9)is symmetric (m=1 halfwaves parallel to compression direction, n=1 halfwaves perpendicular to compression direction) and identical for each determining method. The buckling stress results are listed in the below Tab. 6. The solution described in sec 4, given by analytical approach is very close to the numerical results (maximum difference 6.3 for Elasticity Equations).

Table 6 Summarizing statement of buckling stress values in the 1st buckling mode

	Orthotropic material:			
	Strength of materials equations	Halphin-Tsai equations	Elasticity equations	Isotropic material
Analytical σ_{cr}:	28.9 MPa	38.6 MPa	31.8 MPa	75.9 MPa
Numerical σ_{cr}:	28.6 MPa	38.2 MPa	29.8 MPa	75.9 MPa
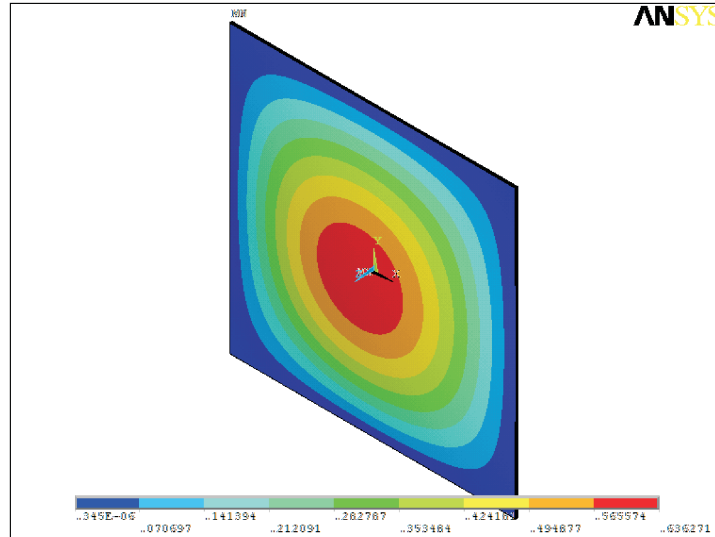
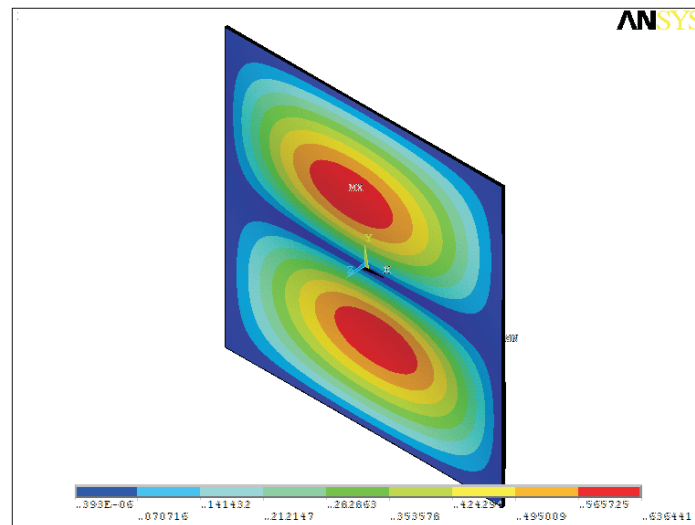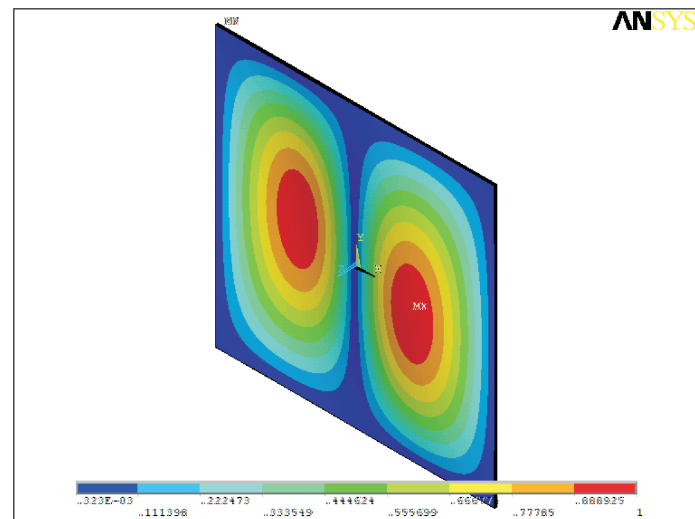**Figure 9** The 1st buckling mode

5.3. Second buckling mode

In the second buckling mode, a sinusoidal (with two amplitudes) form is observed (Fig. 10). For Strength of Materials and Elasticity equations, it is antisymmetric (m=1 halfwaves parallel to compression direction, $n = 2$ halfwaves perpendicular to compression direction), whereas for Halphin–Tsai the form is symmetric ($m = 2$, $n = 1$).

The direction of the waves differs accordingly to the G_{12} value. The buckling value for the Halphin–Tsai Equations is almost the same as for isotropic material. The buckling stress results are listed in the below Tab. 7.

Table 7 Summarizing statement of buckling stress values in the 2nd buckling mode

	Orthotropic material:			
	Strength of materials equations	Halphin-Tsai equations	Elasticity equations	Isotropic material
Numerical σ_{cr}:	55.7 MPa	110.6 MPa	57.0 MPa	118.5 MPa

Figure 10 Strength of Materials and Elasticity Equations- 2nd buckling mode

Figure 11 Halphin–Tsai Equations and Isotropic material- 2nd buckling mode

5.4.   *Third buckling mode*

In the third buckling mode, a sinusoidal form is rotated (in composite structure respectively) (Figs 12 and 13). For Strength of Materials and Elasticity equations it is symmetric ($m = 2$, $n = 1$), whereas for Halphin–Tsai the form is antisymmetric ($m = 1$, $n = 2$).

Only for isotropic material three amplitudes are observed (Fig. 14). The governing equations for orthotropic critical stress are not valid and should be investigated more carefully. The buckling stress results are listed in the below Tab. 8.

Table 8 Summarizing statement of buckling stress values in the 3rd buckling mode

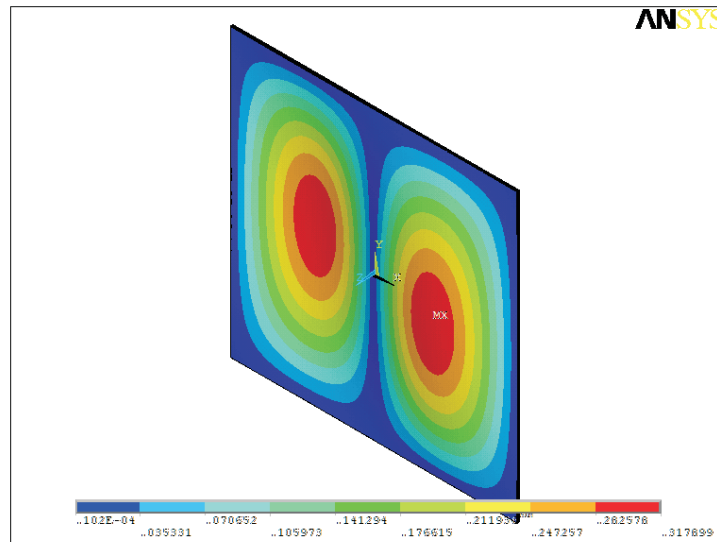|	Orthotropic material:			
	Strength of materials equations	Halphin-Tsai equations	Elasticity equations	Isotropic material
Numerical σ_{cr}:	101.0 MPa	116.6 MPa	103.1 MPa	210.6 MPa

Figure 12 Strength of Materials and Elasticity Equations- 3rd buckling mode
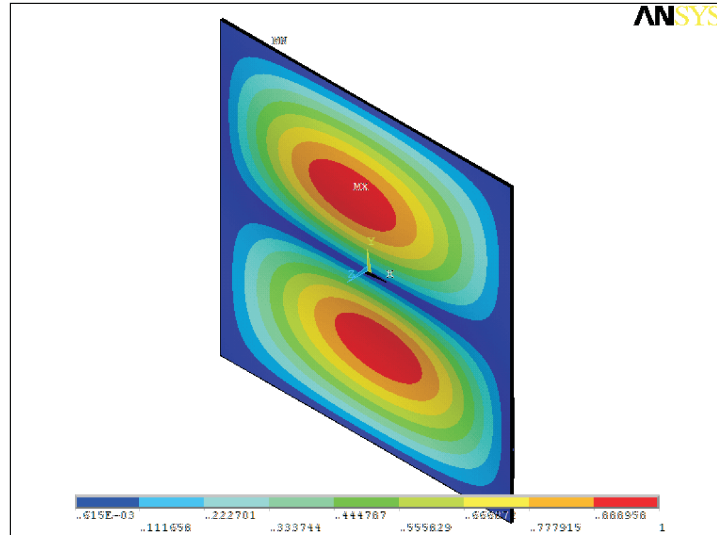
Figure 13 Halphin-Tsai Equations- 3rd buckling mode
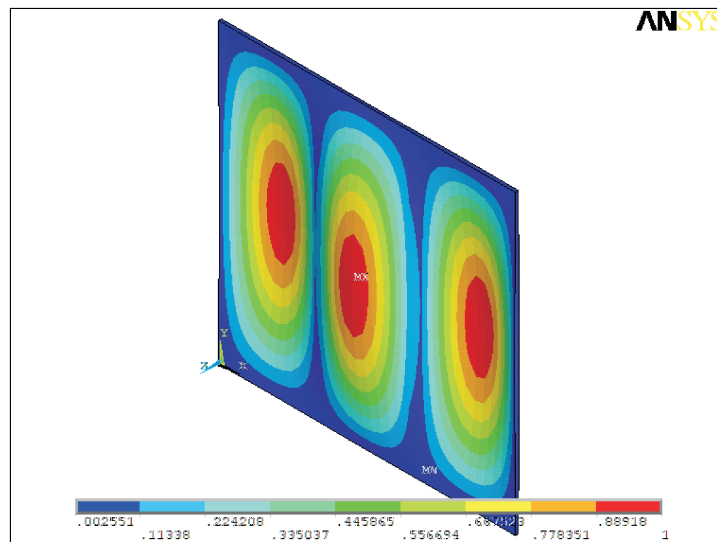

Figure 14 Isotropic Matetial- 3rd critical buckling mode

5.5.   *Fourth buckling mode*

In the fourth buckling mode, a sinusoidal form is observed (four amplitudes) which is similar for each determining method (Fig. 15). The buckling stress results are listed in the below Tab. 9.

Table 9 Summarizing statement of buckling stress values in the 4th buckling mode

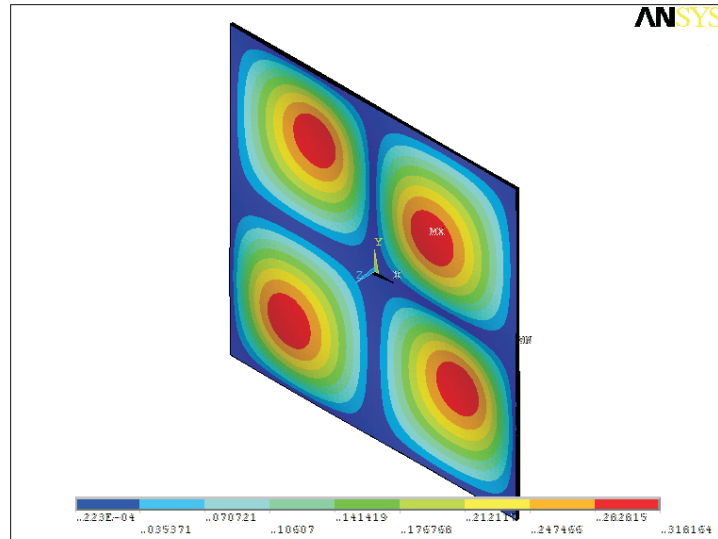|	Orthotropic material:			
	Strength of materials equations	Halphin-Tsai equations	Elasticity equations	Isotropic material
Numerical σ_{cr}:	113.2 MPa	152.4 MPa	118.4 MPa	303.0 MPa

Figure 15 Strength of Materials Theory- 4th critical buckling mode

5.6.   *Results summary. Mass analysis*

The mass analysis for square plates (dimensions: length $a = 500$ mm, width $b = 500$ mm) was carried through. The aim of this was to compare the thicknesses of the boron–epoxy plates h_{co} (properties listed in Tab. 4), alluminium plate h_{al} ($\nu_{al} = 0.32$, $E_{al} = 0.7410^5$ MPa), which buckling stress corresponds to the critical stress in the steel plate (thickness $h_{st} = 5mm$, buckling force $N_{kr} = 189.8$ kN).

Using the relations from sec 4:

$$\chi = \frac{E_{11}(1 + \nu_{21})}{12(1 - \nu_{12}\nu_{21})} + \frac{E_{22}(1 + \nu_{12})}{12(1 - \nu_{12}\nu_{21})} + \frac{G_{12}}{3} \tag{52}$$

$$h_{co} = \sqrt[3]{\frac{bN_{kr}}{\pi^2 \chi}} \tag{53}$$

$$h_{st} = \sqrt[3]{\frac{3N_{kr}(1 - \nu^2)a}{\pi^2 E}} \tag{54}$$

$$h_{al} = \sqrt[3]{\frac{3N_{kr}(1 - \nu_{al}^2)a}{\pi^2 E_{al}}} \tag{55}$$

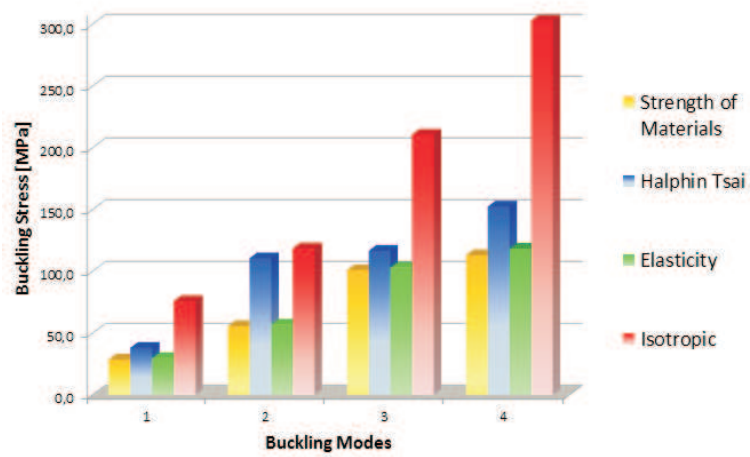the mass corresponds the product of volume and density.

Figure 16 Critical stress in particular modes

Table 10 Numerical stress results summary

Determining method	unit	buckling stress σ_{cr}:			
		1st mode:	2nd mode:	3rd mode:	4th mode:
Orthotropic Material: Boron-epoxy					
Strength of Materials	MPa	28.6	55.7	101.0	113.2
Halphin-Tsai Equations	MPa	38.2	110.6	116.6	152.4
Elasticity Equations	MPa	29.8	57.0	103.1	118.4
Isotropic Material: Steel					
Eigenvalue buckling	MPa	75.9	118.5	210.6	303.0

Table 11 Plate thickness summary

Orthotropic Material: Boron-epoxy				
Strength of Materials	h_{co}	6.9 mm	m_{co}	4.0 kg
Halphin-Tsai Equations	h_{co}	6.3 mm	m_{co}	3.6 kg
Elasticity Equations	h_{co}	6.7 mm	m_{co}	3.9 kg
Isotropic Material: Aluminium				
Eigenvalue Buckling	h_{al}	7.0 mm	m_{co}	4.7 kg
Isotropic Material: Steel				
Eigenvalue Buckling	h_{st}	5.0 mm	m_{co}	9.7 kg
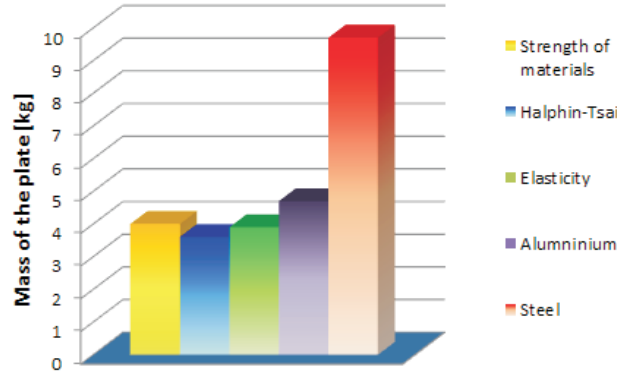
Figure 17 Mass of the plates

The boron–epoxy composite is a very light and resistant material in comparison to steel and aluminium alloys (Tabs 11 and Fig. 17). Depending on determination method, the difference between the composite and aluminium is 0.7–1.1 kg and 4.7–6.1 kg in comparison to steel. For this reason, it is reasonable to use it in low–mass demanding constructions e.g. aircrafts, vessels, cars. Additionally, the increase of the critical stress can be achieved by slight size enlargement. This fact is meaningful for the upgrade of the safety level.

6. Conclusions

The strength properties of the boron–epoxy composite were evaluated using three different methods. For each theory, different values were reached. Additionally, the values of the transverse Young's modulus and in–plane shear modulus play a superior role in creation of symmetric or antisymmetric buckling form. For this reason experimental researches should be done. Although the buckling load for isotropic material is approximately 2 times bigger (than for orthotropic materials), the boron-epoxy composites can be used in well weighted structures.

The author would like to continue the researches in the field of boron-epoxy and boron-aluminium composites with the application in the vehicle railings (different types of support, with stiffening ribbes). The aim of the work is to create a composite assembly with outstandng strength properties, which could be used as reliable and safety upgrading elements in the construction of different means of transport. Experimental tests are predicted to be done in order to create more accurate equations describing the material properties of this interesting material.

References

[1] **Kamiński, M.**: Aeromeeting in Goraszka, **2011**.

[2] **Mack, J.**: Advanced polymer composites, *Mater. Edge*, 18, **1988**.

[3] **Boffy, A.**: Cite de l'Automobile, **2011**.

[4] **Kaw, A.K.**: Mechanics of Composite Materials, *Taylor & Francis Group*, Boca Raton, **2006**.

[5] **Chawla, K.K.**: Fibrous Materials, *Cambridge University Press*, Cambridge, **2005**.

[6] Boeing Co.: Evaluation of Boron/Epoxy doublers for reinforcement of commercial aircraft metallic structures, **1996**

[7] **Weller, T.**: Experimental studies of Graphite–Epoxy and Boron Epoxy angle ply laminates in compression, NASA-CR-145233, September **1977**

[8] http://commons.wikimedia.org: RAAF F111

[9] **Corten, H.T.**: Composite Materials: Testing and Design, ASTM International, Baltimore, **1972**.

[10] **Kołakowski, Z.**: The strength and stability basics of composite plates' construction, *Politechnika Łó dzka*, Łódź, **2008**.

[11] **Jones, R.M.**: Mechanics of Composite Materials, Taylor & Francis Ltd., London, **1999**.

[12] **Timoshenko, S.P.**: Theory of Elastic Stability, *McGraw–Hill Book Company*, INC., London, **1961**.

[13] Ansys: *Release 11.0 Documentation for Ansys*